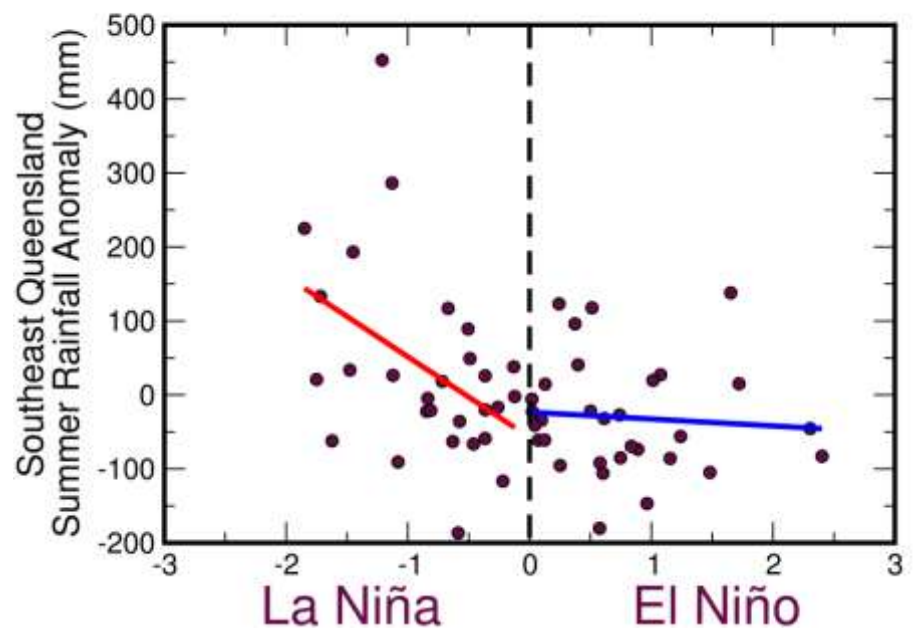


# Asymmetry in ENSO Teleconnection, its Collapse and Impact on South East Queensland Summer Rainfall

Wenju Cai, Peter van Rensch, Tim Cowan and Arnold Sullivan

December 2009

Asymmetry of ENSO Impact, 1950-2008



Urban Water Security Research Alliance  
Technical Report No. 18

Urban Water Security Research Alliance Technical Report ISSN 1836-5566 (Online)  
Urban Water Security Research Alliance Technical Report ISSN 1836-5558 (Print)

The Urban Water Security Research Alliance (UWSRA) is a \$50 million partnership over five years between the Queensland Government, CSIRO's Water for a Healthy Country Flagship, Griffith University and The University of Queensland. The Alliance has been formed to address South-East Queensland's emerging urban water issues with a focus on water security and recycling. The program will bring new research capacity to South-East Queensland tailored to tackling existing and anticipated future issues to inform the implementation of the Water Strategy.

For more information about the:

UWSRA - visit <http://www.urbanwateralliance.org.au/>  
Queensland Government - visit <http://www.qld.gov.au/>  
Water for a Healthy Country Flagship - visit [www.csiro.au/org/HealthyCountry.html](http://www.csiro.au/org/HealthyCountry.html)  
The University of Queensland - visit <http://www.uq.edu.au/>  
Griffith University - visit <http://www.griffith.edu.au/>

Enquiries should be addressed to:

The Urban Water Security Research Alliance  
PO Box 15087  
CITY EAST QLD 4002

Ph: 07-3247 3005; Fax: 07-3405 0373  
Email: Sharon.Wakem@qwc.qld.gov.au

Wenju Cai, Peter van Rensch, Tim Cowan and Arnold Sullivan (2009) *Asymmetry in ENSO Teleconnection, its Collapse and Impact on South East Queensland Summer Rainfall*, Urban Water Security Research Alliance Technical Report No. 18.

### **Copyright**

© 2009 CSIRO. To the extent permitted by law, all rights are reserved and no part of this publication covered by copyright may be reproduced or copied in any form or by any means except with the written permission of CSIRO.

### **Disclaimer**

The partners in the UWSRA advise that the information contained in this publication comprises general statements based on scientific research and does not warrant or represent the accuracy, currency and completeness of any information or material in this publication. The reader is advised and needs to be aware that such information may be incomplete or unable to be used in any specific situation. No action shall be made in reliance on that information without seeking prior expert professional, scientific and technical advice. To the extent permitted by law, UWSRA (including its Partner's employees and consultants) excludes all liability to any person for any consequences, including but not limited to all losses, damages, costs, expenses and any other compensation, arising directly or indirectly from using this publication (in part or in whole) and any information or material contained in it.

### **Cover Image:**

Description: Asymmetry of ENSO Impact, 1950-2008.

## **ACKNOWLEDGEMENTS**

This research was undertaken as part of the South East Queensland Urban Water Security Research Alliance, a scientific collaboration between the Queensland Government, CSIRO, The University of Queensland and Griffith University.

Particular thanks go to CSIRO, The Australian Climate Change Science Program and Ian Smith for his useful comments. In addition, we acknowledge the work undertaken by numerous international modelling groups who provided their model experiments for analysis.

## FOREWORD

Water is fundamental to our quality of life, to economic growth and to the environment. With its booming economy and growing population, Australia's South-East Queensland (SEQ) region faces increasing pressure on its water resources. These pressures are compounded by the impact of climate variability and accelerating climate change.

The Urban Water Security Research Alliance, through targeted, multidisciplinary research initiatives, has been formed to address the region's emerging urban water issues.

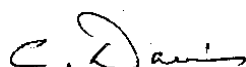
As the largest regionally focused urban water research program in Australia, the Alliance is focused on water security and recycling, but will align research where appropriate with other water research programs such as those of other SEQ water agencies, CSIRO's Water for a Healthy Country National Research Flagship, Water Quality Research Australia, eWater CRC and the Water Services Association of Australia (WSAA).

The Alliance is a partnership between the Queensland Government, CSIRO's Water for a Healthy Country National Research Flagship, The University of Queensland and Griffith University. It brings new research capacity to SEQ, tailored to tackling existing and anticipated future risks, assumptions and uncertainties facing water supply strategy. It is a \$50 million partnership over five years.

Alliance research is examining fundamental issues necessary to deliver the region's water needs, including:

- ensuring the reliability and safety of recycled water systems.
- advising on infrastructure and technology for the recycling of wastewater and stormwater.
- building scientific knowledge into the management of health and safety risks in the water supply system.
- increasing community confidence in the future of water supply.

This report is part of a series summarising the output from the Urban Water Security Research Alliance. All reports and additional information about the Alliance can be found at <http://www.urbanwateralliance.org.au/about.html>.



**Chris Davis**

Chair, Urban Water Security Research Alliance

# CONTENTS

Foreword.....	ii
Executive Summary .....	1
1. Introduction .....	2
2. Model Experiments, Reanalysis and Observations .....	3
3. Results from C mip3 20th Century Experiments and Targeted Runs .....	4
4. Asymmetry in Enso and Enso Modoki Impacts .....	6
5. Breakdown of Rainfall Teleconnection since 1980 .....	10
6. Multidecadal Fluctuations in Teleconnection.....	12
7. Conclusions .....	15
Glossary.....	16
References .....	17

# LIST OF FIGURES

Figure 1	(a) Australian summer (December, January and February, or DJF) rainfall trends over the period 1950-2008 ( $\text{mm year}^{-1}$ ). The bordered area indicates the SEQ region. (b) SEQ summer rainfall time series together with trend lines over 1950-1979 (red), 1980-2008 (blue) and 1950-2008 (green). .....	2
Figure 2	One standard deviation anomaly patterns obtained by linearly regressing observed grid-point SST onto, (a) detrended NINO3.4 and (b) detrended EMI, and then multiplying by the one standard deviation value of the index. Dashed (solid) green contours indicate positive (negative) correlations significant at the 90% confidence level. ....	4
Figure 3	SEQ rainfall trends in terms of percentage of climatology from the observed (1950-2008, blue), from IPCC 20th century climate model experiments (1950-1999, red), and from the CSIRO Mk3A model with different forcing scenarios (green) (see text for details). The error bars indicate the standard error of the linear regression of the ensemble-mean. ....	5
Figure 4	Scatter plot of detrended SEQ summer rainfall anomalies versus (a) detrended NINO3.4 over the period 1950-2008, (b) detrended EMI over the period 1950-2008, and (c) detrended SOI over the period 1900-2008, with correlations and slopes of the linear fits conducted separately using samples corresponding to positive and negative values of the indices. ....	6
Figure 5	Anomaly patterns obtained by linearly regressing, onto negative (La Niña, left column) and positive (El Niño, right column) NINO3.4 values (note the colour reversal for ease of comparison), anomalies of detrended grid-point rainfall (a and d, $\text{mm } ^\circ\text{C}^{-1}$ ), OLR (b and e, $\text{Wm}^{-2} \text{ } ^\circ\text{C}^{-1}$ ), and vertical velocity at 500mB (c and f, $\text{Pa s}^{-1} \text{ } ^\circ\text{C}^{-1}$ , negative = upward motion). Dashed (solid) green contours indicate positive (negative) correlations significant at the 90% confidence level. ....	8
Figure 6	The same as Figure 5, but using the ENSO Modoki index. ....	9
Figure 7	(a) Scatter plot of detrended SEQ summer rainfall anomalies versus detrended NINO3.4, with linear fits using samples with positive and negative NINO3.4 values, and anomaly patterns obtained by linearly regressing grid-point rainfall (b, $\text{mm } ^\circ\text{C}^{-1}$ ) and OLR (c, $\text{Wm}^{-2} \text{ } ^\circ\text{C}^{-1}$ ) onto negative NINO3.4 values (La Niña) using corresponding samples for the period 1950-1979. Panels (d)-(f), the same as (a)-(c) but for the period 1980-2008. Dashed (solid) green contours indicate positive (negative) correlations significant at the 90% confidence level. ....	10
Figure 8	The same as Figure 7, but using the ENSO Modoki index. ....	11
Figure 9	Time series of correlation, using a 13-year sliding-window, of SEQ summer rainfall with (a) NINO3.4 and (b) EMI over the period 1900-2008, together with time series of an annual IPO index (in red). Based on the definition described by Parker et al. (2007). ....	12
Figure 10	Anomaly pattern associated with the IPO obtained by linear regression using detrended NCEP anomalies since 1948 of (a) OLR ( $\text{Wm}^{-2} \text{ } ^\circ\text{C}^{-1}$ ), and (b) surface zonal wind ( $\text{m s}^{-1} \text{ } ^\circ\text{C}^{-1}$ ). Dashed (solid) green contours indicate positive (negative) correlations significant at the 90% confidence level. ....	13
Figure 11	Scatter plot of detrended SEQ summer rainfall anomalies versus (a) detrended NINO3.4, and (b) detrended EMI, with separate linear fits using samples with positive and negative values of the indices for the period 1921-1950. ....	14
Figure 12	Scatter plot of detrended SEQ summer rainfall anomalies versus detrended NINO3.4 from the second half of the 20th century experiments based on 24 IPCC AR4 models. Separate linear fits using samples with positive and negative values of the index are also shown. ....	15

## EXECUTIVE SUMMARY

South East Queensland (SEQ) austral summer rainfall has been declining since around the 1980s, however the associated process is not understood. We show that the reduction is not simulated by the majority of current climate models forced with climate change, nor in experiments with individual anthropogenic forcing factors.

We then examine a possible contribution from natural variability, and find that El Niño-Southern Oscillation (ENSO) is a rainfall-generating mechanism for the region because of an asymmetry in the ENSO impact. The associated La Niña events induce a statistically significant increase in rainfall in SEQ and the stronger the La Niña event, the more the rainfall produced. El Niño events bring reduced rainfall to SEQ. However, there is no statistically significant relationship between the magnitude of the El Niño event and the amount of rainfall reduction.

A similar asymmetry exists in the impact from ENSO Modoki, suggesting that ENSO Modoki as an entity is similarly rain-conducive for the region. The asymmetry fluctuates on a multi-decadal time scale and is sensitive to the multi-decadal mean position of the tropical Pacific main convection centre, particularly the South Pacific Convergence Zone (SPCZ) during austral summer.

Since about 1980, this mechanism no longer operates due to a breakdown in the impacts from La Niña and La Niña Modoki events, contributing to the observed rainfall reduction in SEQ. The research showed that the influence from the SPCZ originated from further west during the pre-1980 period than that during the post-1980 period. This is consistent with a post-1980 eastward shift in the Walker circulation and the associated convection centre. Because of this shift, despite a westward swing during La Niña events, the impact barely reaches SEQ.

A similar breakdown occurred in both event types before 1950. This indicates that multi-decadal variability alone could potentially be responsible for the recent SEQ rainfall decline. However, it is not possible to preclude a contribution from climate change, which unfortunately cannot be assessed because most climate models do not simulate the observed ENSO-rainfall teleconnection over the SEQ region.

# 1. INTRODUCTION

Austral summer (December – February) rainfall over SEQ (150.50°E-154.50°E, 20.50°S-30.50°S), denoted by a border in Figure 1a, accounts for most of the annual total, and its variability is thought to be dominated by ENSO. Over recent decades, there has been a decline in summer rainfall, which is manifested as a reduction in heavy rainfall events with much lower monthly totals since 1980 (Figure 1b), contributing to about a 20% reduction since 1950, amid significant reductions over other Australian regions (Figure 1a) (Cai et al. 2001; Alexander et al. 2007). Numerous studies have examined the decline over southwest Western Australia (e.g., Smith et al. (2000); Hope et al. (2006); Cai et al. (2005); Cai and Cowan (2006)), and across southeast Australia (Cai and Cowan 2008), but few have focused on the reduction over SEQ.

Cai et al. (2001) suggest that the decline is consistent with an El Niño-like warming pattern in response to global warming, as simulated by a climate model (Meehl and Washington 1996). However, such an El Niño-like rainfall response is now in question (Collins and The CMIP Modelling Groups 2005; Vecchi et al. 2006), although the associated eastward shift and a weakening of the climatological Walker circulation are simulated by most models used for the Intergovernmental Panel on Climate Change (IPCC) Fourth Assessment Report (AR4). On the other hand, SEQ summer rainfall is a part of an Australia-wide annual total rainfall influenced by multi-decadal variability (Power et al. 1999). Thus the mechanism leading to the reduction remains unclear. Are the reduction and the associated processes captured by the IPCC AR4 20th century experiments? Is the reduction driven by multi-decadal variability or climate change?

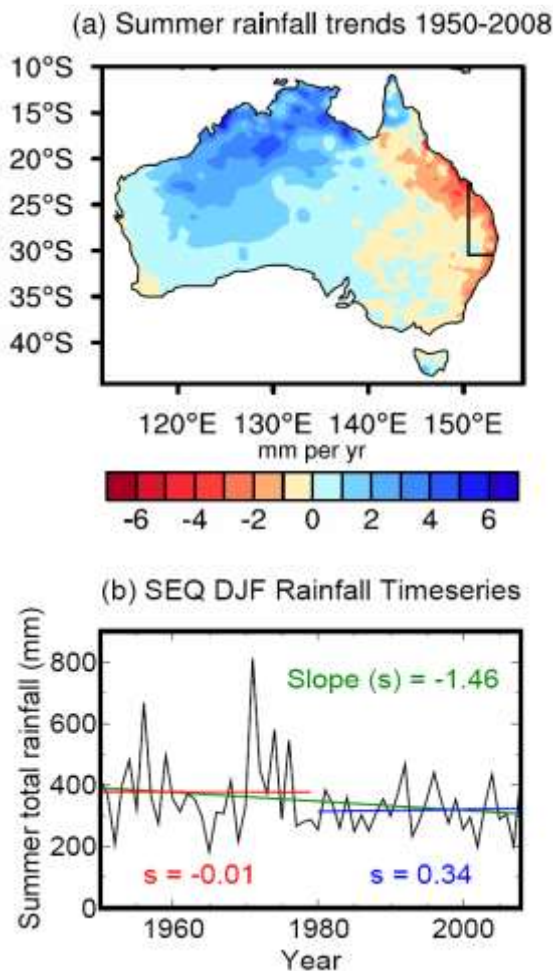


**Figure 1** (a) Australian summer (December, January and February, or DJF) rainfall trends over the period 1950-2008 ( $\text{mm year}^{-1}$ ). The bordered area indicates the SEQ region. (b) SEQ summer rainfall time series together with trend lines over 1950-1979 (red), 1980-2008 (blue) and 1950-2008 (green).

Another issue is whether the observed reduction is induced by a different ENSO pattern, referred to as ENSO Modoki (Ashok et al. 2007), which has the anomaly centre at the Dateline rather than in the central-eastern Pacific and occurs more frequently in recent decades. During an El Niño Modoki event, there are two anomalous Walker circulation cells in the troposphere, instead of the single-celled pattern of the conventional El Niño. The core rising branch of the double-celled Walker circulation is located over the central equatorial Pacific, and the associated western descending branch is situated over Indonesia and northern Australia and is therefore more effective in suppressing Australian rainfall. In spring, this explains the inter-event difference in the impact on Australia rainfall between the 2002 El Niño (a dominantly Modoki event, with extremely dry conditions across Australia) and the 1997 episode (conventional El Niño, with little rainfall reduction in Australia) (Wang and Hendon 2007). However, the situation in autumn is different in that only La Niña Modoki events have a statistically significant impact over Australia (Cai and Cowan 2009). The influence in summer has not been clear. We explore the impact of ENSO Modoki in summer, and examine if it is a catalyst for the SEQ rainfall reduction.

## 2. MODEL EXPERIMENTS, REANALYSIS AND OBSERVATIONS

We analyse the 20th century experiments from 24 models submitted as part of the IPCC AR4, comprising a total of 75 simulations made available through the Third Climate Model Intercomparison Project (CMIP3). Model names and details are listed in Table 1 of Cai et al. (2009) with references to further documentation. Two-thirds of models have multiple ensemble members. A total of 44 experiments include a stratospheric ozone forcing component, while the rest do not, allowing stratification into groups: with and without ozone depletion.

Because ozone forcing may not be the only difference between these two groups, and as all models include an anthropogenic aerosol forcing in one form or another, we have also analysed a series of targeted multi-member ensemble experiments with the CSIRO Mk3A model (Rotstayn et al. 2007) designed to isolate the impacts of individual forcing factors. The impact of ozone depletion (four ensemble members) and greenhouse gases-only (four ensemble members) in these targeted experiments are realised by forcing the model with a time-evolving forcing alone. The impact of an anthropogenic aerosol forcing is obtained by comparing two sets of experiments (eight ensemble members each) with and without increasing aerosols, both in the presence of all other forcing factors.

As will be shown (section 2), the majority of models and targeted model experiments do not simulate the observed rainfall reduction. If these models are perfect, it would imply that multi-decadal variability plays a role in forcing the observed reduction. Given that ENSO is the dominant driver, we examine whether the changing properties, the associated multi-decadal mean state in the Pacific (Wang 1995), and ENSO Modoki plays a part.

To this end, an updated version of the Hadley Centre's Global Sea Ice and sea surface temperature (SST) reanalysis (Rayner et al. 2003), covering data since 1870, is used to construct an ENSO index (NINO3.4) (170°W-120°W, 5°S-5°N), ENSO Modoki index (EMI) and their associated circulation patterns. The EMI is defined following Ashok et al. (2007), i.e.,

$$EMI = [SSTA]_A - 0.5 \times ([SSTA]_B + [SSTA]_C)$$

where the square brackets represent the area-averaged SST anomalies for the regions A (165°E-140°W, 10°S-10°N), B (110°W-70°W, 15°S-5°N), and C (125°E-145°E, 10°S-20°N), respectively.

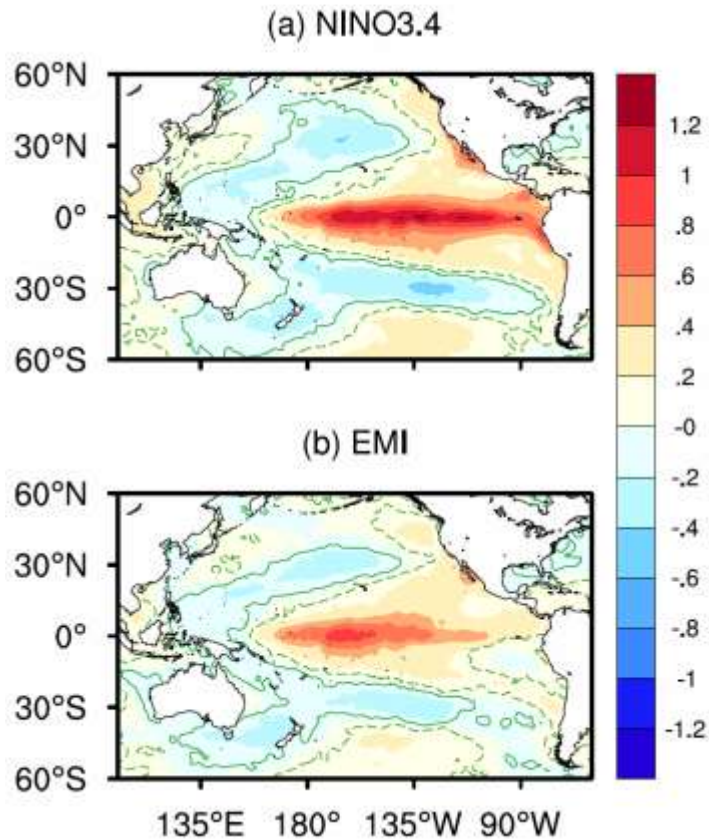


**Figure 2** One standard deviation anomaly patterns obtained by linearly regressing observed grid-point SST onto, (a) detrended NINO3.4 and (b) detrended EMI, and then multiplying by the one standard deviation value of the index. Dashed (solid) green contours indicate positive (negative) correlations significant at the 90% confidence level.

As a means of providing information for the later sections, Figure 2 displays the anomaly pattern associated with ENSO and the ENSO Modoki, through a regression of SST onto their relative indices (e.g. NINO34 and EMI). Because summer is the season in which both ENSO and ENSO Modoki mature, SST anomalies associated with either type are similar, well developed, and occupy almost the entire equatorial Pacific. Indeed the correlation between the EMI and NINO3.4 (both detrended) for this season using samples since 1950 is rather high, at 0.65. In other seasons (e.g., austral spring and autumn), the anomaly pattern associated with the EMI displays a warming anomaly in the Dateline region but cooling anomalies both sides. In the case of summer, the cooling in the eastern Pacific is weak (Figure 2b), suggesting that there is no pronounced double-celled Walker circulation. As will be shown later, the impact from ENSO Modoki on SEQ summer rainfall is similar to that of conventional ENSO.

Also deployed are reanalyses from the National Center for Environmental Prediction (Kalnay et al. 1996) and observed Australian rainfall since 1900 from the Australian Bureau of Meteorology Research Centre. As we are interested in variability, monthly and seasonal anomalies are referenced to the climatological mean over the period 1950–2008 and are linearly detrended, unless otherwise stated.

### 3. RESULTS FROM CMIP3 20TH CENTURY EXPERIMENTS AND TARGETED RUNS

Is the summer rainfall reduction reproduced by climate models? For all but one of the experiments, the ensemble-mean trend from each model over 1950-1999 is calculated (the Mk3A ozone ensemble is calculated over 1961-2000, as the model experiment starts at 1961). The uncertainty range of the trend is estimated as the standard error of the linear regression fit on the ensemble-mean data.

Several results emerge for SEQ (Figure 3). Firstly, only four models (red crosses, GFDL-CM2.1, MIROC3.2(hires), INM-CM3.0, IPSL-CM4) produce a rainfall decline over SEQ that is comparable to the observed. Secondly, the observed summer rainfall reduction is not generated in an all-model ensemble mean (orange cross), which, as an entity, contains all climate change forcing factors, such as greenhouse gases, aerosols, and stratospheric ozone depletion. Thirdly, results from targeted experiments forced by ozone depletion only (green circle), or a comparison between the CMIP3 model groups with and without ozone depletion (orange circles), show that ozone depletion has little impact. Finally, increasing aerosols, if anything, tend to increase SEQ summer rainfall, although the increase is very small (green crosses).

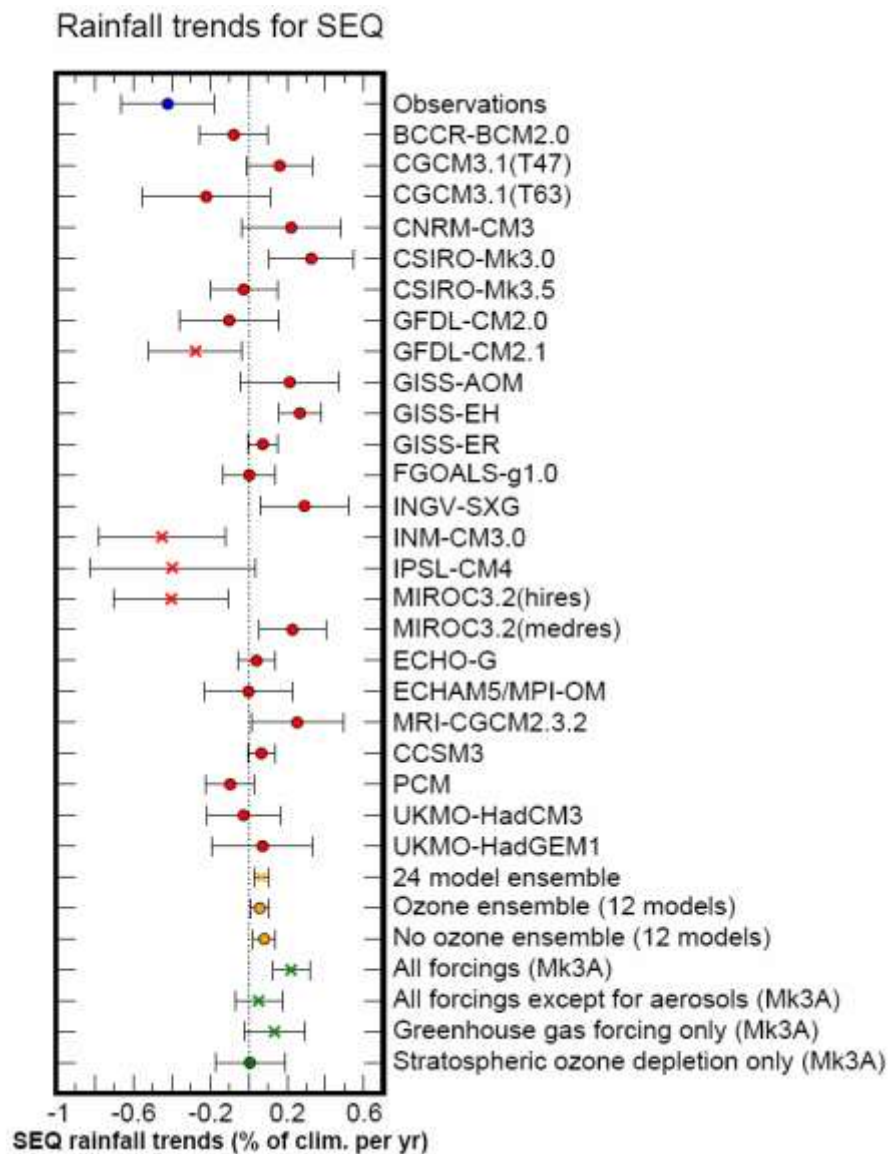


**Figure 3** SEQ rainfall trends in terms of percentage of climatology from the observed (1950-2008, blue), from IPCC 20th century climate model experiments (1950-1999, red), and from the CSIRO Mk3A model with different forcing scenarios (green) (see text for details). The error bars indicate the standard error of the linear regression of the ensemble-mean.

Thus, the observed rainfall decrease in SEQ is not produced by the majority of models, nor is attributable to any individual climate change forcing factor. Two possible implications are: firstly, climate change has little impact and much of the observed reduction is driven by internal variability. Secondly, climate change has an impact, but models do not capture the associated process. In either case, it is important to understand the mechanism of the observed rainfall reduction; therefore we focus on the impact from ENSO from an observational perspective.

#### 4. ASYMMETRY IN ENSO AND ENSO MODOKI IMPACTS

What is the impact from the ENSO cycle as an entity? ENSO can be divided into two distinct phases, El Niño and La Niña. Figure 4a depicts the relationship of SEQ summer rainfall with each phase through a linear fit showing a slope and a correlation using samples with positive and negative values of the indices. A distinct asymmetry emerges. A significant correlation exists during La Niña conditions, meaning that SEQ summer rainfall increases as La Niña amplitude increases, with a sensitivity of approximately  $109 \text{ mm } ^\circ\text{C}^{-1}$  cooling in NINO3.4 (a negative slope). Yet such an ENSO-rainfall teleconnection is not evident during El Niño conditions. Although rainfall tends to decrease during El Niño conditions, the influence is not statistically significant (correlation of -0.08), meaning that stronger El Niño events do not statistically generate a greater rainfall reduction. The asymmetry is reproduced using the EMI (Figure 4b) though with a higher sensitivity, suggesting that the impacts from the two types of ENSO in this season are similar. The asymmetry is also generated using an atmospheric index of ENSO, the Southern Oscillation Index (SOI), from anomalies since 1900 (Figure 4c).

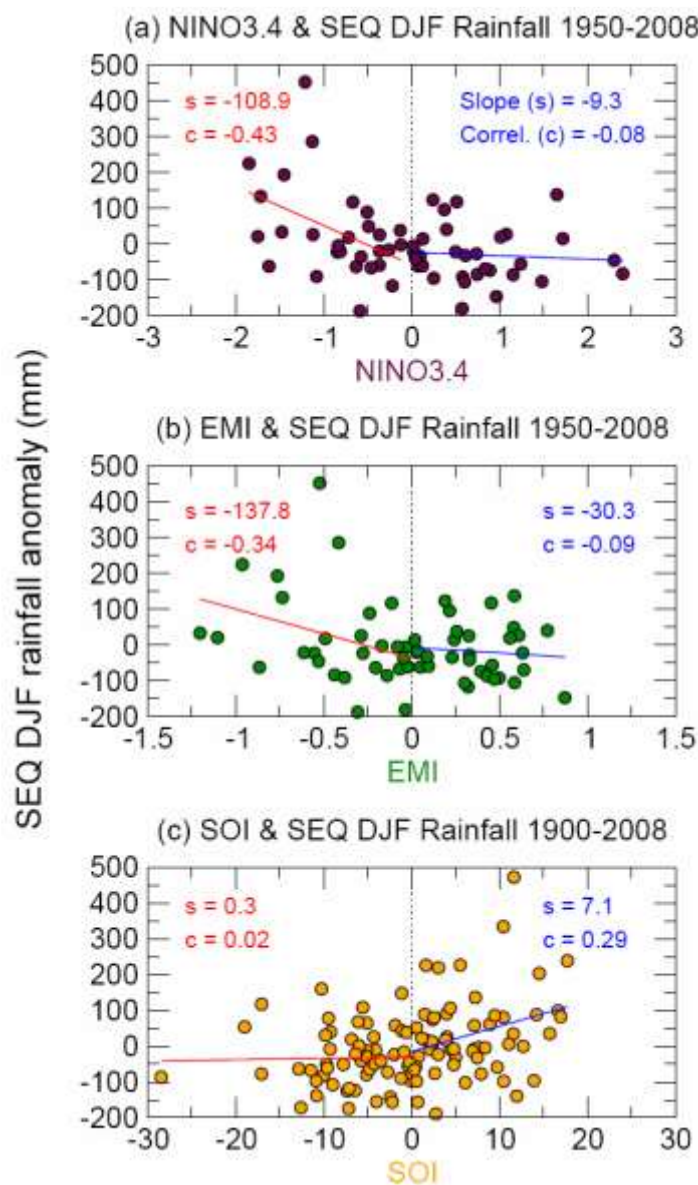
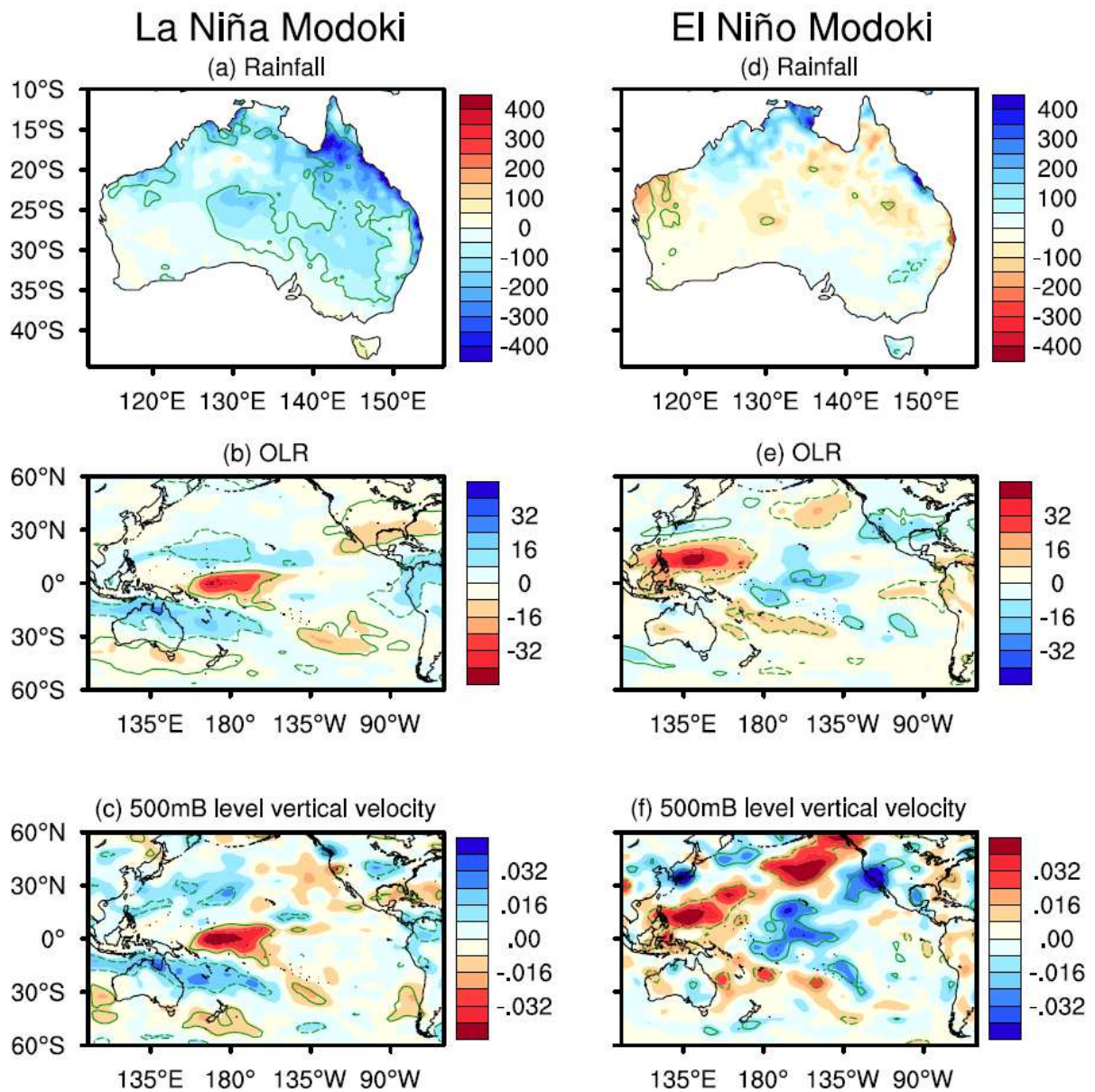


Figure 4 Scatter plot of detrended SEQ summer rainfall anomalies versus (a) detrended NINO3.4 over the period 1950-2008, (b) detrended EMI over the period 1950-2008, and (c) detrended SOI over the period 1900-2008, with correlations and slopes of the linear fits conducted separately using samples corresponding to positive and negative values of the indices.

A similar analysis is conducted by regressing grid-point circulation anomalies onto the NINO3.4 index, using samples with negative (La Niña) and positive (El Niño) NINO3.4 values. Maps of the associated regression coefficients (shaded) and correlation coefficients (contours) show that during La Niña conditions (Figure 5a), the rainfall influence is broad in scale over eastern Australia, but completely disappears during El Niño conditions (Figure 5d). One cause could be that atmospheric circulation anomalies that lead to rainfall declines cannot reduce rainfall below zero, i.e., by more than the climatological mean (~330 mm for SEQ during summer). However, the reduction in SEQ rainfall in El Niño years is generally far smaller. Another potential cause is the appreciable longitudinal shift in the main heating anomalies, indicating a shift in the mean convection centre between La Niña and El Niño events (Hoerling et al. 1997). This has been invoked to explain a nonlinear teleconnection with temperature and rainfall over North America. Below, we illustrate that such a zonal shift together with a difference in the response of the South Pacific Convergence Zone (SPCZ) is responsible for the asymmetry over SEQ.

ENSO-rainfall teleconnections are generated mainly through movements of the tropical convergence zones from their seasonal mean positions. During La Niña, the warm pool expands meridionally and shifts westwards. In association, convection reduces over the central equatorial Pacific, reflecting a westward migration of the west Pacific convergence zone, as seen in the regression/correlation between NINO3.4 with outgoing longwave radiation (OLR, Figure 5b). This is accompanied by an enhanced convection extending from the equatorial latitudes towards the subtropical Pacific in both sides of the equator, indicative of a poleward expansion of the Intertropical Convergence Zone (ITCZ) and the SPCZ. In austral summer, the impact from the SPCZ is particularly important, as it reflects anomalies associated with a high-intensity warm hemisphere convergence zone. The anomaly extends into eastern Australia, leading to an increase in rainfall over SEQ (blue, Figure 5a). Anomalies of vertical velocities display attendant uplift motions where convection intensifies (Figure 5c). Most importantly, the extent of the SPCZ's southward expansion and the intensity in convection is proportional to the amplitude of La Niña. This is why SEQ summer rainfall increases with La Niña amplitude.

Anomaly patterns associated with El Niño are generally similar, but maximum regression and correlation coefficients in the tropical Pacific are situated further to the east (Figures 5e and 5f). As cooling in the west Pacific and warming in the central and eastern equatorial Pacific lead to more uniform total SSTs, a merger of these major convergence zones ensues. The ITCZ and SPCZ move towards the equator, and together with the convergence zone over the west Pacific, they migrate eastward, where the strongest warm SST anomalies develop. Once the merged convergence zone (i.e., the main heating region) moves sufficiently away from the west Pacific, El Niño intensity becomes irrelevant for its impacts over SEQ. Thus, the ENSO-rainfall teleconnection over SEQ is highly sensitive to an eastward shift in the mean convection centre.



**Figure 5** Anomaly patterns obtained by linearly regressing, onto negative (La Niña, left column) and positive (El Niño, right column) NINO3.4 values (note the colour reversal for ease of comparison), anomalies of detrended grid-point rainfall (a and d, mm °C<sup>-1</sup>), OLR (b and e, Wm<sup>-2</sup> °C<sup>-1</sup>), and vertical velocity at 500mB (c and f, Pa s<sup>-1</sup> °C<sup>-1</sup>, negative = upward motion). Dashed (solid) green contours indicate positive (negative) correlations significant at the 90% confidence level.

A similar asymmetry in circulation is generated using the EMI, as illustrated in Figure 6. In particular, there is a strong teleconnection during La Niña Modoki phases as a result of convective heating. This is associated with a broader and stronger SPCZ that is situated over the western Pacific and intensifies with La Niña Modoki amplitudes, and a weak teleconnection during El Niño Modoki phases as convergence moves sufficiently eastwards.

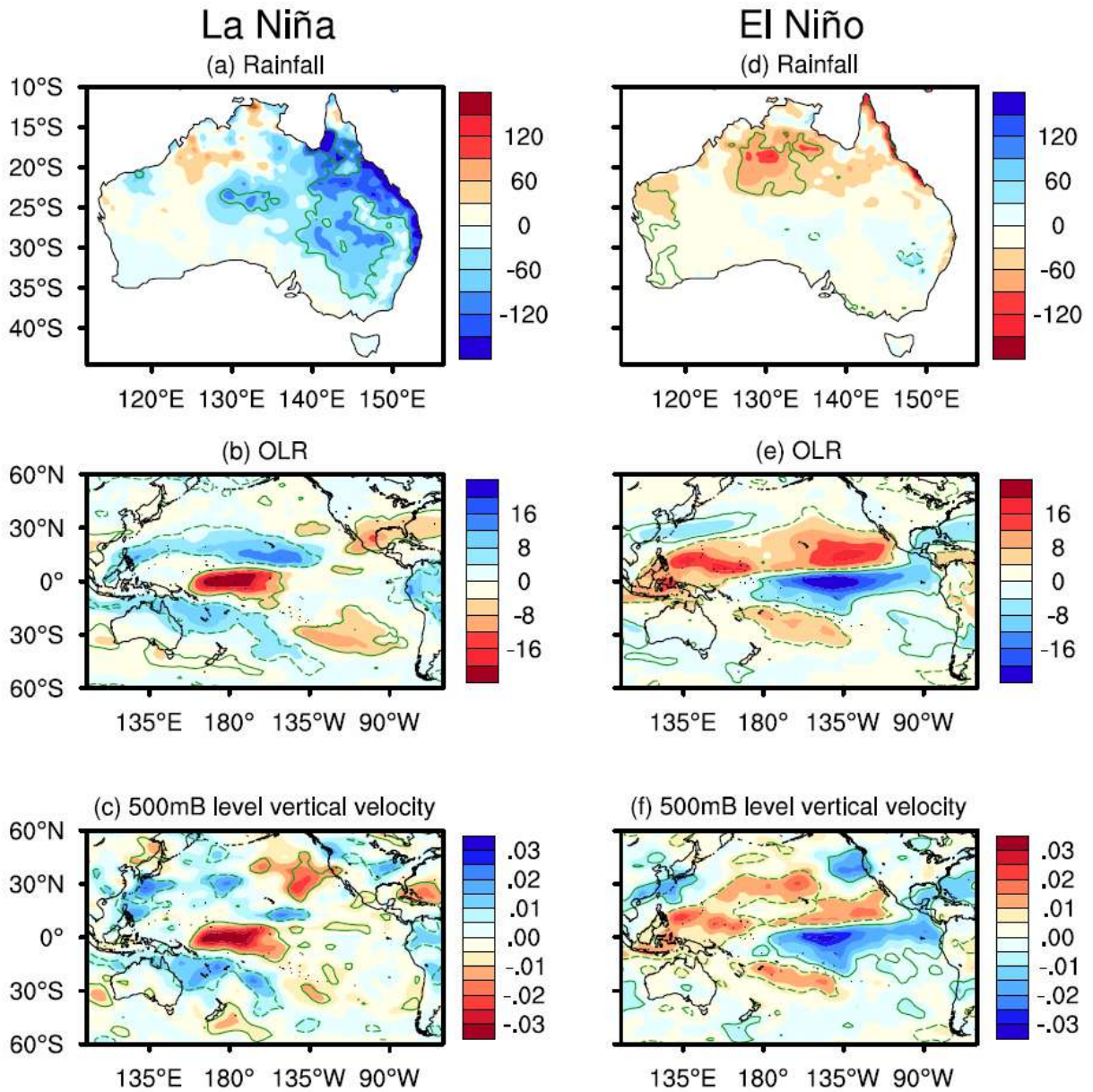


**Figure 6** The same as Figure 5, but using the ENSO Modoki index.

The asymmetry means that the ENSO or ENSO Modoki cycle as an entity is conducive for SEQ summer rainfall, because the rainfall increase during La Niña years more than offsets the reduction during El Niño phases. Indeed the ENSO cycle is an important mechanism of rainfall generation for the region. Recent studies suggest that the frequency of La Niña events has been on a decline, whereas the frequency of El Niño has been increasing, based on a count using the SOI (Power and Smith 2007). This would cause a summer rainfall reduction over SEQ, but using NINO3.4 and defining a La Niña as when its amplitude exceeds a one-standard deviation value, only a slight decline in the number of La Niña events is evident throughout the same period. As we will show in Section 5, since the 1980s, the ENSO-rainfall teleconnection over SEQ collapses, with La Niña or La Niña Modoki events no longer exerting a significant influence. This appears to be the main cause behind the SEQ summer rainfall reduction.

## 5. BREAKDOWN OF RAINFALL TELECONNECTION SINCE 1980

The ENSO-rainfall teleconnection for SEQ is not stationary but time evolving. Splitting samples used in Figure 4a into two periods, 1950-1979 and 1980-2008, we see that the asymmetry within the ENSO-rainfall teleconnection is time-dependent (Figures 7a and 7d). As expected, both periods show El Niño correlations with SEQ summer rainfall that are not statistically significant. However, a very strong correlation is seen for the pre-1980 La Niña events, above the 98% confidence level, reflecting La Niña-induced strong rainfall events (for the 90% confidence level, with 15 independent samples, a correlation coefficient of 0.41 is required). By contrast, for the post-1980 period the impact from La Niña events is not significant and the asymmetry between the impact of La Niña and El Niño is barely visible. Thus, the asymmetry shown in Figures 4 and 5 predominantly exists in the pre-1980 period, and since 1980 there is a complete breakdown in the ENSO-rainfall teleconnection over SEQ, meaning that the summer rainfall generating process no longer operates. This is reflected in the rainfall time series (Figure 1b), showing that since the 1980s there have been far fewer large seasonal totals.

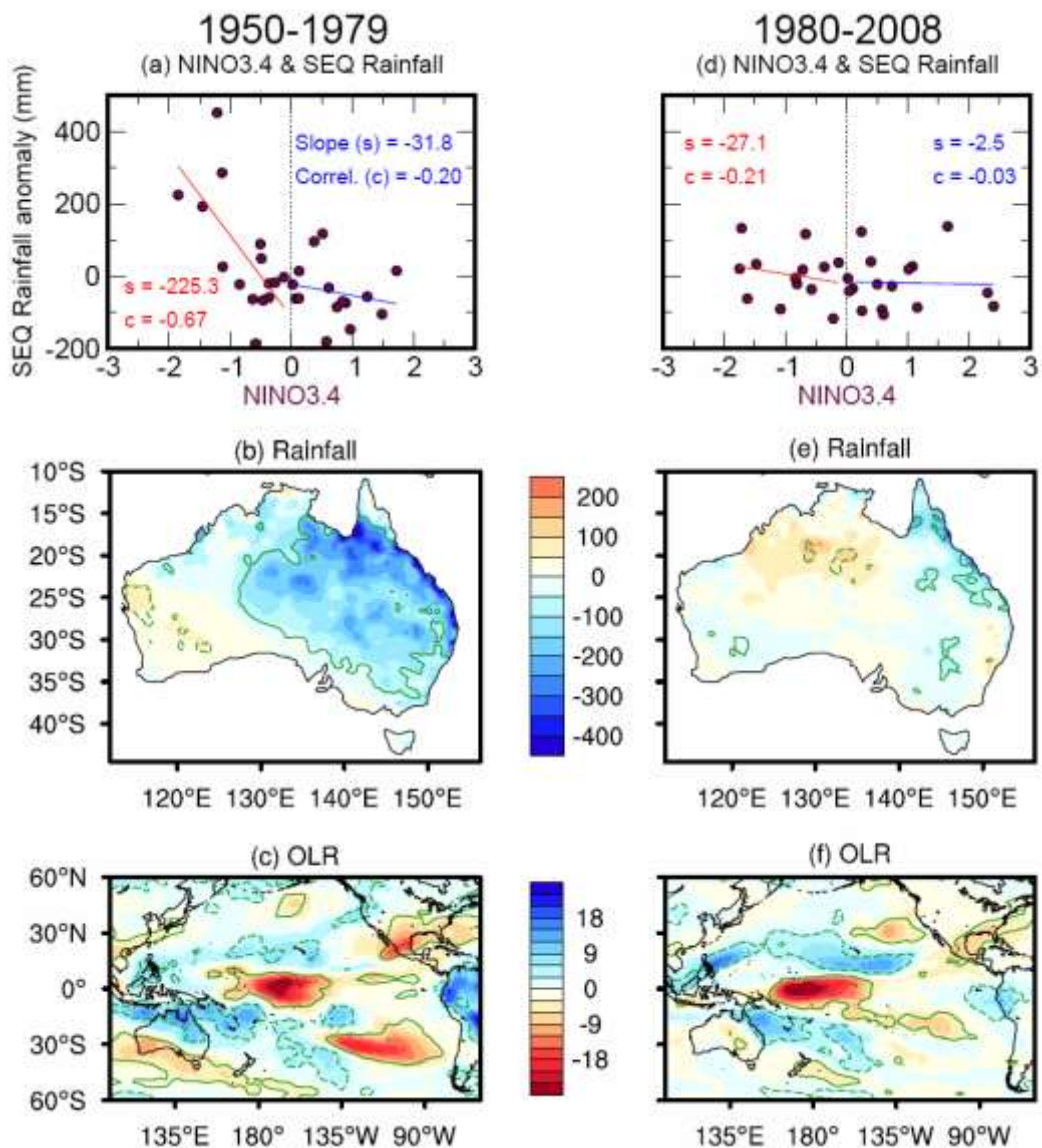


**Figure 7** (a) Scatter plot of detrended SEQ summer rainfall anomalies versus detrended NINO3.4, with linear fits using samples with positive and negative NINO3.4 values, and anomaly patterns obtained by linearly regressing grid-point rainfall (b, mm °C<sup>-1</sup>) and OLR (c, Wm<sup>-2</sup> °C<sup>-1</sup>) onto negative NINO3.4 values (La Niña) using corresponding samples for the period 1950-1979. Panels (d)-(f), the same as (a)-(c) but for the period 1980-2008. Dashed (solid) green contours indicate positive (negative) correlations significant at the 90% confidence level.

Comparing the OLR regression and correlation patterns with La Niña events for the pre- and post-1980 periods (Figures 7c and 7f), one finds that their overall patterns actually resemble each other. However, a remarkable difference exists in the warm hemisphere. The influence from the SPCZ originates from further west during the pre-1980 period than that during the post-1980 period, consistent with a post-1980 eastward shift in the Walker circulation and the associated convection centre. Because of the shift, despite a westward swing during La Niña events, the impact barely reaches SEQ (Figure 7e and 7f).

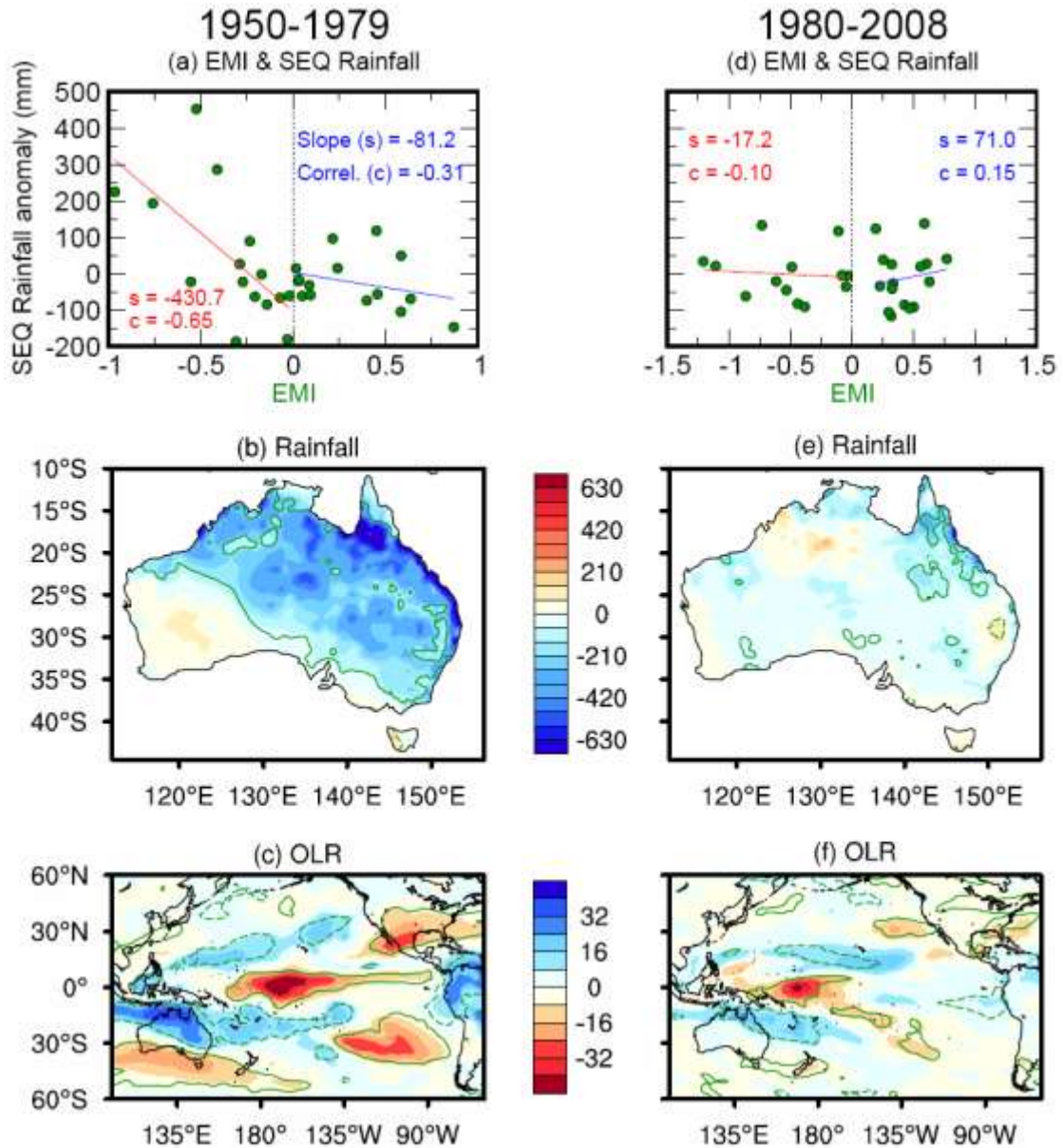


**Figure 8** The same as Figure 7, but using the ENSO Modoki index.

The fluctuations in the asymmetry during the pre- and post-1980 periods and the associated circulation differences between the two phases generally carry over to ENSO Modoki (Figure 8). One important feature worth noting is that SEQ summer rainfall appears to be rather sensitive to La Niña Modoki amplitude, more so than to La Niña amplitude.

## 6. MULTIDECADAL FLUCTUATIONS IN TELECONNECTION

The breakdown since 1980 is apparent in the time series of correlations of the SEQ summer rainfall with NINO3.4 or the EMI using a 13-year sliding window (Figure 9), showing another period of low correlation centred at around 1935. The evolution co-varies with the Interdecadal Pacific Oscillation (IPO), similar to the correlation between ENSO and all-Australia rainfall (Power et al. 1999). During an IPO high phase, the multi-decadal-mean circulations resemble those associated with El Niño.

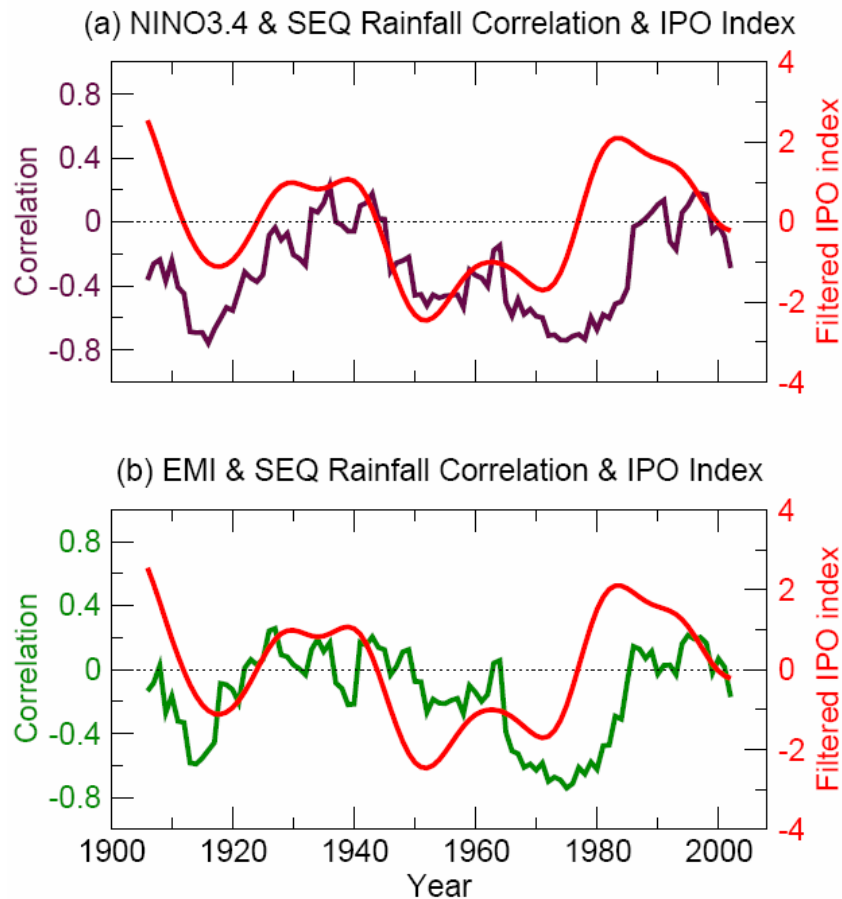


**Figure 9** Time series of correlation, using a 13-year sliding-window, of SEQ summer rainfall with (a) NINO3.4 and (b) EMI over the period 1900-2008, together with time series of an annual IPO index (in red). Based on the definition described by Parker et al. (2007).

The SST anomaly pattern associated with the IPO, obtained by linear regression using National Centre for Environmental Prediction (NCEP) detrended anomalies since 1948 (the year NCEP reanalysis coverage starts), features a warming in the east and a cooling in the west, though broader in scale than that associated with ENSO on an interannual basis. In response, convection activities shift to the east (Figure 10a). In association, equatorial surface easterly winds, which feed into the ascending motion, decrease showing strong westerly anomalies. These provide multi-decadal-mean conditions upon which interannual ENSO or ENSO Modoki oscillates. But even during La Niña phases, when the convection centre is shifted closest to Australia, the impact is small. The interannual ENSO rainfall correlation over SEQ therefore breaks down completely, reinforcing the notion that the ENSO-rainfall teleconnection over SEQ is highly sensitive to the multi-decadal-mean condition.

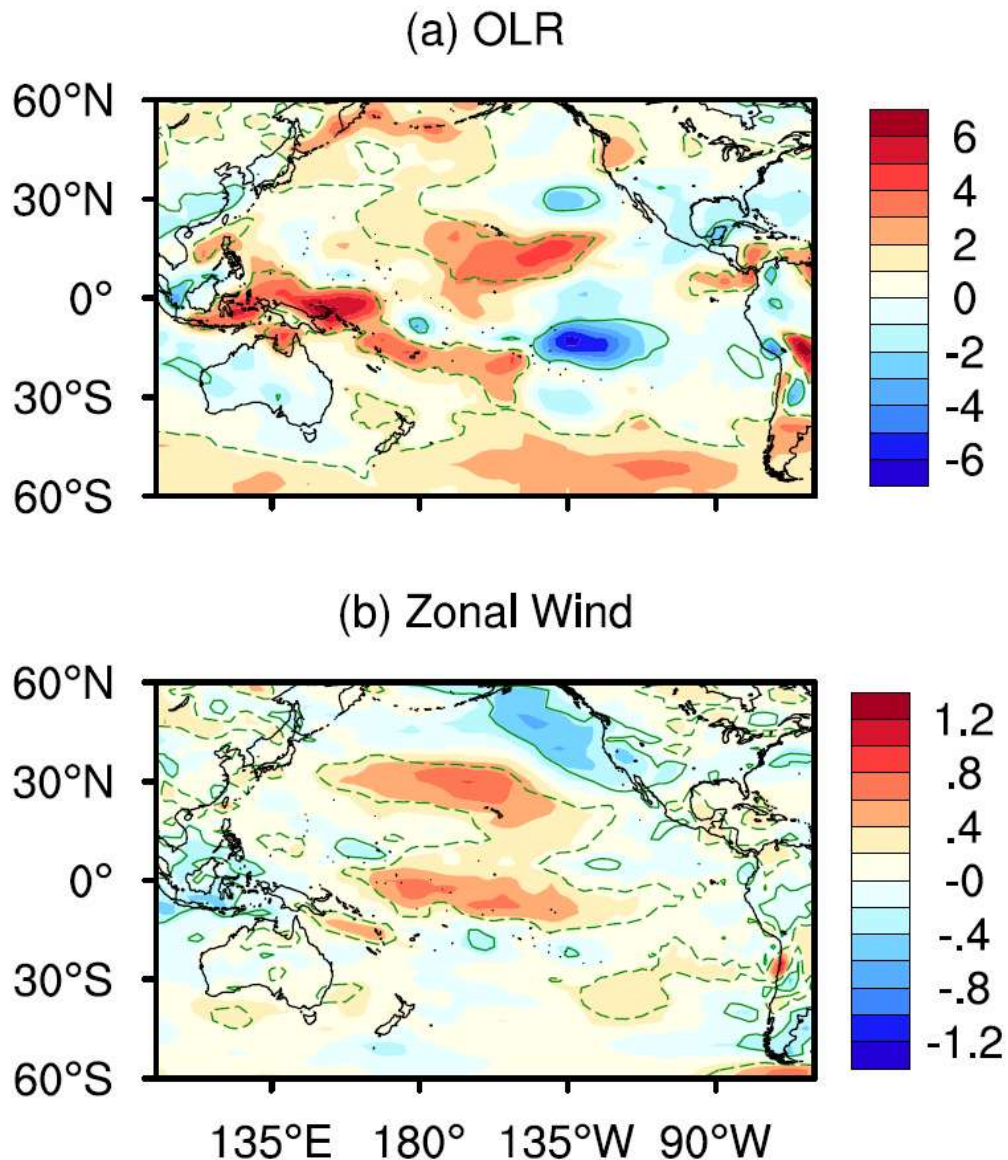


**Figure 10** Anomaly pattern associated with the IPO obtained by linear regression using detrended NCEP anomalies since 1948 of (a) OLR ( $\text{Wm}^{-2} \text{ } ^\circ\text{C}^{-1}$ ), and (b) surface zonal wind ( $\text{m s}^{-1} \text{ } ^\circ\text{C}^{-1}$ ). Dashed (solid) green contours indicate positive (negative) correlations significant at the 90% confidence level.

A similar breakdown in the influence from La Niña or La Niña Modoki occurred during the previous low-correlation period (i.e., about 1935) (Figure 11). Likewise, there is no significant correlation during La Niña conditions, nor during El Niño phases. That the rainfall reduction is due to the breakdown is further reinforced by the fact that there is actually an increase in the amplitude of La Niña Modoki since the 1980s which would have induced a stronger rainfall if the teleconnection still operated. In terms of NINO3.4, there is no obvious trend that could explain the SEQ summer rainfall reduction either.

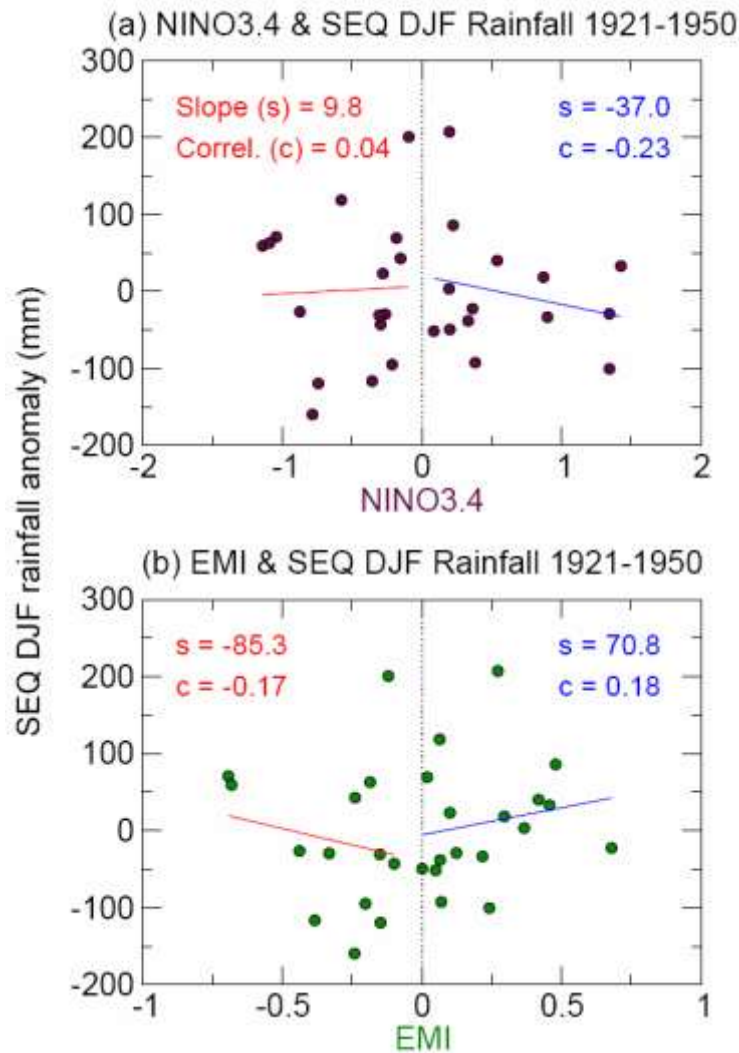


**Figure 11** Scatter plot of detrended SEQ summer rainfall anomalies versus (a) detrended NINO3.4, and (b) detrended EMI, with separate linear fits using samples with positive and negative values of the indices for the period 1921-1950.

The fact that the breakdown in the teleconnection was also seen around 1935 suggests that multi-decadal variability has the potential to generate the recent breakdown and the rainfall decline. However, this does not preclude a contribution from climate change, which is usually distilled through an aggregation of multi-model outputs to remove the component driven by climate variability. Unfortunately, this is not possible because most climate models suffer from a cold tongue bias in the equatorial Pacific, with a warm pool and the associated mean convection centre located too far west (Cai et al. 2009). As a result, an unrealistic ENSO-rainfall teleconnection exists over Australia, with a significant correlation over western Australia rather than eastern Australia (Cai et al. 2009). For example, only four out of 24 CMIP3 models produce a correlation between NINO3.4 and SEQ summer rainfall that is comparable to or greater than the observed (see Figure 6a of Cai et al. (2009)). Another consequence of the model bias is that the asymmetry in the ENSO-rainfall teleconnection is not generated (Figure 12), in part because of the weak rainfall teleconnection. The absence of an ENSO-rainfall teleconnection over SEQ means that it is not possible to use these models to assess the role of climate change in the recent teleconnection breakdown, and hence in the rainfall reduction.

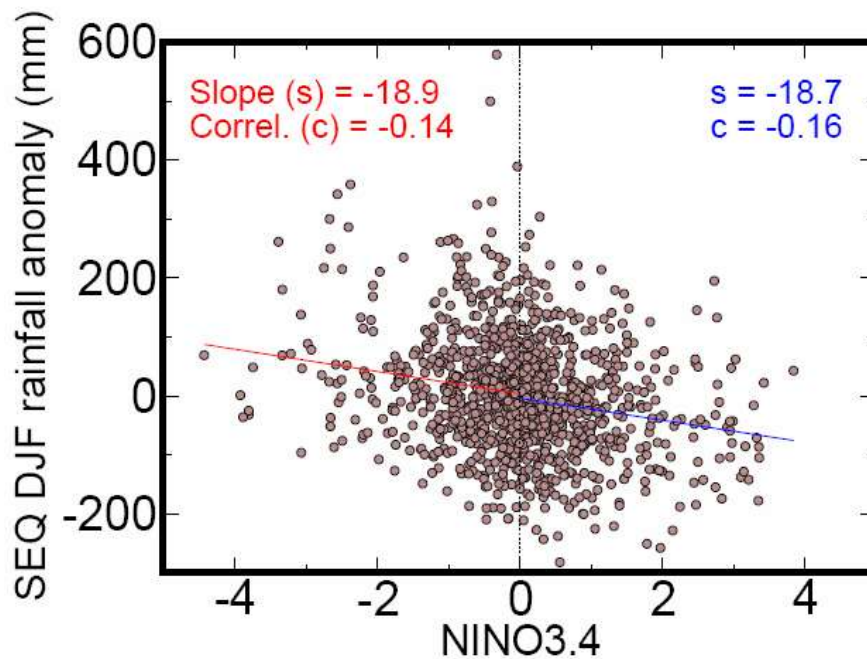


Figure 12 Scatter plot of detrended SEQ summer rainfall anomalies versus detrended NINO3.4 from the second half of the 20th century experiments based on 24 IPCC AR4 models. Separate linear fits using samples with positive and negative values of the index are also shown.

## 7. CONCLUSIONS

This study addressed what drives the observed SEQ summer rainfall decline. We showed that the decline is not simulated by the majority of climate models forced by climate change, nor is it attributable to any individual climate change forcing factors such as greenhouse gases, ozone depletion and anthropogenic aerosols. We therefore examined climate variability as a possible driver and showed that the ENSO-rainfall teleconnection is a rainfall-generating mechanism for the SEQ region.

La Niña events induce a statistically significant increase in rainfall in SEQ and the stronger the La Niña event, the more the rainfall produced. El Niño events bring reduced rainfall to SEQ, however there is no statistically significant relationship between the magnitude of the El Niño event and the amount of rainfall reduction.

Such an asymmetry undergoes multi-decadal fluctuations and is sensitive to the multi-decadal mean position of the tropical Pacific main convection centre, particularly the SPCZ during austral summer. The research showed that the influence from the SPCZ originated from further west during the pre-1980 period than that during the post-1980 period, consistent with a post-1980 eastward shift in the Walker circulation and the associated convection centre. Because of this shift, despite a westward swing during La Niña events, the impact barely reaches SEQ.

Since 1980, there is a complete breakdown in the teleconnection with La Niña over the region, such that La Niña events no longer bring strong rainfall events, contributing to the rainfall reduction. A similar asymmetry exists in the impact from ENSO Modoki, suggesting that ENSO Modoki as an entity is similarly rain-conducive for the SEQ region. The resemblance in the impact arises because in this season there is little difference in the circulation anomalies between the two types of ENSO. A similar breakdown is seen in the early 20<sup>th</sup> century, indicating that multi-decadal variability has the potential to cause the recent decline in rainfall. However, this does not exclude a co-impact from climate change, because the majority of climate models do not simulate the observed ENSO-rainfall teleconnection over the SEQ region. Thus, it is essential for climate models to realistically simulate this rainfall teleconnection before they are used in attribution studies in ENSO-affected regions.

## **GLOSSARY**

<b>AR4</b>	Fourth Assessment Report (of the IPCC)
<b>CMIP3</b>	Third Coupled Model Intercomparison Project
<b>CSIRO Mk3A</b>	Commonwealth Scientific and Industrial Research Organisation Mark 3A general circulation model
<b>DJF</b>	Austral summer (December, January and February)
<b>EMI</b>	El Niño Modoki Index
<b>ENSO</b>	El Niño-Southern Oscillation
<b>IPCC</b>	Intergovernment Panel on Climate Change
<b>IPO</b>	Interdecadal Pacific Oscillation
<b>ITCZ</b>	Intertropical Convergence Zone
<b>NCEP</b>	National Centre for Environmental Prediction
<b>OLR</b>	Outgoing longwave radiation
<b>SEQ</b>	South East Queensland
<b>SOI</b>	Southern Oscillation Index
<b>SPCZ</b>	South Pacific Convergence Zone
<b>SST</b>	Sea surface temperature

## REFERENCES

- Alexander, L. V., P. Hope, D. Collins, B. Trewin, A. Lynch, and N. Nicholls, 2007, Trends in Australia's climate means and extremes: a global context. *Aust. Met. Mag.*, 56, 1–18.
- Ashok, K., S. K. Behera, S. A. Rao, H. Weng, and T. Yamagata, 2007, El Niño Modoki and its possible teleconnection. *J. Geophys. Res.*, 112, C11007, doi:10.1029/2006JC003798.
- Cai, W. and T. Cowan, 2006, SAM and regional rainfall in IPCC AR4 models: can anthropogenic forcing account for southwest Western Australian winter rainfall reduction? *Geophys. Res. Lett.*, 33, L24708, doi:10.1029/2006GL028037.
- Cai, W. and T. Cowan, 2008, Dynamics of late autumn rainfall reduction over southeastern Australia. *Geophys. Res. Lett.*, 35, L09708, doi:10.1029/2008GL033727.
- Cai, W. and T. Cowan, 2009, La Niña Modoki impacts Australia autumn rainfall variability. *Geophys. Res. Lett.*, 36, L12805, doi:10.1029/2009GL037885.
- Cai, W., G. Shi, and Y. Li, 2005, Multidecadal fluctuations of winter rainfall over southwest Western Australia simulated in the CSIRO Mark 3 coupled model. *Geophys. Res. Lett.*, 32, L12701, doi:10.1029/2005GL022712.
- Cai, W., A. Sullivan, and T. Cowan, 2009, Rainfall teleconnections with Indo-Pacific variability in the WCRP CMIP3 models. *J. Climate*, 22, 5046–5071.
- Cai, W., P. H. Whetton, and A. B. Pittock, 2001, Fluctuations of the relationship between ENSO and northeast Australian rainfall. *Clim. Dyn.*, 17, 421–432.
- Collins, M. and The CMIP Modelling Groups, 2005, El Niño- or La Niña-like climate change? *Clim. Dyn.*, 24, 89104, doi:10.1007/s00382-004-0478-x.
- Hoerling, M. P., A. Kumar, and M. Zhong, 1997, El Niño, La Niña, and the nonlinearity of their teleconnections. *J. Climate*, 10, 1769–1786.
- Hope, P., W. Drosowsky, and N. Nicholls, 2006, Shifts in the synoptic systems affecting southwest Western Australia. *Clim. Dyn.*, 26, 751–764.
- Kalnay, E., et al., 1996, The NCEP/NCAR 40-Year Reanalysis Project. *Bull. Amer. Meteor. Soc.*, 3, 437–471.
- Meehl, G. and W. Washington, 1996, El Niño-like climate change in a model with increased atmospheric CO<sub>2</sub> concentrations. *Nature*, 382, 56–60.
- Parker, D., C. Folland, A. Scaife, J. Knight, A. Colman, P. Baines, and B. Dong, 2007, Decadal to multidecadal variability and the climate change background. *J. Geophys. Res.*, 112, D18115, doi:10.1029/2007JD008411.
- Power, S., C. Folland, A. Colman, and V. Mehta, 1999, Inter-decadal modulation of the impact of ENSO on Australia. *Clim. Dyn.*, 15, 319–324.
- Power, S. B. and I. N. Smith, 2007, Weakening of the Walker Circulation and apparent dominance of El Niño both reach record levels, but has ENSO really changed? *Geophys. Res. Lett.*, 34, doi:10.1029/2007/GL030854.
- Rayner, N. A., D. E. Parker, E. B. Horton, C. K. Folland, L. V. Alexander, D. P. Rowell, E. C. Kent, and A. Kaplan, 2003, Global analyses of sea surface temperature, sea ice, and night marine air temperature since the late nineteenth century. *J. Geophys. Res.*, 108, doi:10.1029/2002JD002670.
- Rotstayn, L. D., et al., 2007, Have Australian rainfall and cloudiness increased due to the remote effects of the Asian anthropogenic aerosols? *J. Geophys. Res.*, 112, D09202, doi: 10.1029/2006JD007712.
- Smith, I. N., P. McIntosh, T. J. Ansell, C. J. C. Reason, and K. L. McInnes, 2000, Southwest Western Australian winter rainfall and its association with Indian Ocean climate variability. *Int. J. Climatol.*, 20, 1913–1930.
- Vecchi, G. A., B. J. Soden, A. T. Wittenberg, I. M. Held, A. Leetmaa, and M. J. Harrison, 2006, Weakening of tropical Pacific atmospheric circulation due to anthropogenic forcing. *Nature*, 441, 73–76.
- Wang, B., 1995, Interdecadal changes in El Niño onset in the last four decades. *J. Climate*, 8, 267–285.
- Wang, G. and H. H. Hendon, 2007, Sensitivity of Australian rainfall to inter-El Niño variations. *J. Climate*, 20, 4211–4226.

# Urban Water Security Research Alliance

